THE SPECTRAL STRUCTURE OF TES PROCESSES

DAVID L. JAGERMAN
BENJAMIN MELAMED

NEC USA, Inc.
C&C Research Laboratories
4 Independence Way
Princeton, New Jersey 08540

Abstract

TES (*Transform-Expand-Sample*) is a versatile class of stochastic sequences consisting of marginally uniform autoregressive schemes with modulo-1 reduction, followed by various transformations. TES modeling aims to fit a TES model to empirical records by simultaneously capturing both first-order and second-order properties of the empirical data.

In this paper we study the spectral properties of general TES processes and their component innovation sequences, thus generalizing the results reported in Jagerman and Melamed [9]. We derive formulas for the power spectral density function and the spectral distribution function which are suitable for efficient numerical computation, and exemplify them for TES processes with uniform and exponential marginals. The results contribute to the understanding of TES sequences as models of autocorrelated sequences, particularly in a Monte Carlo simulation context.

Keywords and Phrases: TES Processes, Stochastic Processes, Spectrum, Spectral Density, Spectral Analysis

1 INTRODUCTION

TES (*Transform-Expand-Sample*) processes constitute a broad class of autocorrelated stochastic sequences with versatile autocorrelation functions (monotone, oscillatory, alternating), and a broad qualitative variety of sample paths. They can be interpreted geometrically as random walks on a circle of circumference 1, referred to as the *unit circle*. TES sequences are easily generated on a computer and their autocorrelation function is readily computed numerically. An important application of TES processes is to model autocorrelated arrivals and services in queueing systems; see Livny et al. [15] for a simulation study on the effect of autocorrelation on mean waiting time statistics. TES processes were introduced in Melamed [16], and their transition and autocorrelation structures were studied in some detail in Jagerman and Melamed [7, 8]; see the next section for a brief survey. A spectral analysis (Hamming [6]) of basic TES processes appeared in Jagerman and Melamed [9]. This paper extends the scope of Jagerman and Melamed [9] to general TES processes.

Let $\{X_n\}_{n=0}^{\infty}$ be a stationary discrete time real process with common mean μ_X and common variance $0 < \sigma_X^2 < \infty$. The second-order structure of $\{X_n\}$ is captured by the autocorrelation function $\rho_X(\tau)$, given by

$$\rho_X(\tau) \;=\; \frac{E[X_n\, X_{n+\tau}] \;-\; \mu_X^2}{\sigma_X^2}, \quad \tau \geq 0, \tag{1.1}$$

independent of $n \geq 0$. Spectral analysis provides an alternative characterization of the second-order structure of a stochastic process (see Grenander and Rosenblatt [5]). The principal tool here is the *normalized spectral density function* (*spectral density*, for short), which can be represented in terms of the autocorrelation function as

$$s_X(\omega) \;=\; \frac{1}{\pi}\left[1 \;+\; 2\sum_{\tau=1}^{\infty} \rho_X(\tau)\, \cos(\tau\omega)\right], \quad 0 \leq \omega < \pi. \tag{1.2}$$

Related to it, is the *normalized spectral distribution function* $S_X(\omega)$ (*spectral distribution*, for short), with the representation

$$S_X(\omega) \;=\; \frac{1}{\pi}\left[\omega \;+\; 2\sum_{\tau=1}^{\infty} \rho_X(\tau)\, \frac{\sin(\tau\omega)}{\tau}\right], \quad 0 \leq \omega < \pi. \tag{1.3}$$

The two are related by

$$s_X(\omega) \;=\; \frac{d}{d\omega} S_X(\omega), \tag{1.4}$$

and S_X satisfies $S_X(0) = 0$ and $S(\pi) = 1$. The Herglotz theorem (Grenander and Rosenblatt [5]) leads to the inverse relations

$$\rho_X(\tau) \;=\; \int_0^\pi \cos(\tau\omega)\, dS_X(\omega) \;=\; \int_0^\pi s_X(\omega)\, \cos(\tau\omega)\, d\omega, \quad \tau = 0, 1, \ldots \tag{1.5}$$

Eqs. (1.2) and (1.3) are given in terms of the radian frequency $0 \le \omega \le \pi$. However, it is customary to plot the spectral density in terms of the Hertz frequency $0 \le f \le 0.5$, where $\omega = 2\pi f$. This necessitates a scaling of $s_X(\omega)$ and $S_X(\omega)$ to corresponding $s_X^*(f)$ and $S_X^*(f)$, such that

$$s_X^*(f) \;=\; 2\,\pi\, s_X(2\pi f), \quad S_X^*(f) \;=\; 2\,\pi\, S_X(2\pi f), \quad 0 \le f \le 0.5, \tag{1.6}$$

in order that $\int_0^{0.5} s_X^*(f)\, df = 1$.

For empirically-observed autocorrelations $\hat\rho_X(0),\ \hat\rho_X(1), \ldots, \hat\rho_X(m)$, the use of (1.2) for constructing an approximation of $s_X(\omega)$ is not suitable. Even if the values of $\hat\rho_X(\tau)$ were exact, a partial sum of the Fourier series for $s_X(\omega)$ would not maintain the non-negative character of $s_X(\omega)$ and, hence, could yield inappropriate approximations. One uses, instead, the Cesaro mean of the partial sums (Cox and Lewis [2]), viz.

$$s_X^{(m)}(\omega) \;=\; \frac{1}{\pi}\left[1 \,+\, 2\sum_{\tau=1}^{m}\left(1 - \frac{\tau}{m+1}\right)\hat\rho_X(\tau)\, \cos(\tau\omega)\right], \quad 0 \le \omega \le \pi, \tag{1.7}$$

in which $s_X^{(m)}(\omega)$ is taken to approximate $s_X(\omega)$. The function $s_X^{(m)}$ provides an overdamped approximation and has the further property that if the $\hat\rho_X(\tau)$ values are exact, then $s_X^{(m)}(\omega) \ge 0$. The spectral distribution counterpart of Eq. (1.7) is the approximation $S_X^{(m)}$, defined as

$$S_X^{(m)}(\omega) \;=\; \frac{1}{\pi}\left[\omega \,+\, 2\sum_{\tau=1}^{m}\left(1 - \frac{\tau}{m+1}\right)\hat\rho_X(\tau)\, \frac{\sin(\tau\omega)}{\tau}\right], \quad 0 \le \omega \le \pi. \tag{1.8}$$

From an informational point of view, the autocorrelation function and spectral density function of a process are equivalent, since each may be transformed into the other. However, the manner in which information is presented is quite different. The autocorrelation function (1.1) is a measure of linear dependence, often used as a proxy for general dependence in a time series. The spectral density and spectral distribution functions describe the distribution of power with respect to frequency and are routinely used for this purpose by electrical engineers, mainly in the context of signal processing. Periodicities present in the original process are evidenced by concentrations of power at discrete points — the point spectrum, while what may be described as "quasi-periodicities" are reflected in the spectrum as local maxima. Electronics and communications engineers use spectral analyzer devices to obtain the spectrum directly in order to study the effect of transformations (filters) on the original process. When the signal (data) is offered as input to a device which acts as a bounded time-invariant transformation, knowledge of the input spectrum allows ready computation of the output spectrum in terms of the transfer impedance function (eigenvalues) of the transformation. Further, the second-order theory of filtering and prediction is based on the spectrum of the data. The spectral density (power spectrum) is also used in engineering to analyze the prominence of periodic components present in a signal. In general, a strong peak suggests the presence of a distinguished periodic component at the corresponding frequency, whereas a flat spectrum indicates the lack of such periodic components. A peak at frequency 0 (DC component) implies an asymmetric constant average level of the signal.

The relevance of the frequency domain approach to random traffic offered to queueing systems has been recently highlighted by the work of S.Q. Li and co-workers [13, 14, 20, 21]. This work has demonstrated the importance of second-order characterizations of input traffic on queueing, loss and output traffic statistics; more specifically, it suggests that the low frequencies of the spectrum dominate these performance measures. An application of the frequency domain approach to congestion control of high-speed networks appears in Sheng and Li [20].

In this paper, we study the spectral properties of TES processes in order to gain insight into their (random) periodic structure. The paper is organized as follows. Section 2 reviews some definitions and results pertaining to TES processes. Sections 3 and 4 derive efficient numerically-computable formulas for the spectral functions of two classes of TES processes, called TES^+ and TES^-, respectively. Section 5 investigates when compatible TES^+ and TES^- processes have mirror-image spectral densities. Finally, Section 6 illustrates the spectral densities and the mirror-image property through various examples, and wraps up the paper with concluding remarks.

2 TES PROCESSES

A detailed study of the qualitative behavior of TES sample path realizations and their attendant autocorrelation functions appears in Melamed [16] and in Jagerman and Melamed [7, 8]. This section contains a brief review of TES processes relevant to this paper.

Throughout this paper, the Laplace Transform of a function $f(x)$ is always denoted by appending a tilde to the function symbol, i.e., $\tilde{f}(s) = \int_{-\infty}^{\infty} e^{-sx} f(x)\, dx$. The modulo-1 (fractional part) operator, $\langle \cdot \rangle$, is defined for any real x by $\langle x \rangle = x - \max\{\text{integer } n : \; n \leq x\}$. Finally, the indicator function of set A is denoted by 1_A.

Let $\{V_n\}_{n=1}^{\infty}$ be a sequence of i.i.d. (independent identically distributed) random variables, called the *innovation* sequence, with marginal density f_V. Let $U_0 \sim$ Uniform$(0, 1)$ be independent of the innovations $\{V_n\}$. Two classes of TES sequences, denoted TES$^+$ and TES$^-$ and collectively called *background* sequences, give rise to two types of processes, $\{U_n^+\}_{n=0}^{\infty}$ and $\{U_n^-\}_{n=0}^{\infty}$ respectively, defined on a common probability space by

$$U_n^+ = \begin{cases} U_0, & n = 0 \\ \langle U_{n-1}^+ + V_n \rangle, & n > 0 \end{cases} \tag{2.1}$$

and

$$U_n^- = \begin{cases} U_n^+, & n \text{ even} \\ 1 - U_n^+, & n \text{ odd} \end{cases} \tag{2.2}$$

The superscript notation in Eqs. (2.1)-(2.2) is motivated by the fact that $\{U_n^+\}$ and $\{U_n^-\}$ can generate lag-1 autocorrelations in the range $[0, 1]$ and $[-1, 0]$, respectively. In fact, Eq. (2.2) implies $\rho_U^-(\tau) = (-1)^\tau \rho_U^+(\tau)$, where $\rho_U^+(\tau)$ and $\rho_U^-(\tau)$ are the autocorrelation functions corresponding to $\{U_n^+\}$ and $\{U_n^-\}$, respectively. From now on, we shall always append plus or minus superscripts to other mathematical objects associated with $\{U_n^+\}$ and $\{U_n^-\}$ in a natural way. However, when the distinction between TES$^+$ and TES$^-$ is not important, the superscript will be omitted. Lemma 1 in Jagerman and Melamed [7] ensures that both $\{U_n^+\}$ and $\{U_n^-\}$ have Uniform$(0, 1)$ marginals.

A Lebesgue-measurable transformation D from [0,1) to the reals is called a *distortion*. D is used to transform a TES sequence $\{U_n\}$ with uniform marginals on $[0,1)$ (a fact denoted by $U_n \sim$ Uniform$(0,1)$) to a sequence $\{X_n\}$, such that $X_n = D(U_n)$, where the X_n have a common marginal F. When $D = F^{-1}$, then D coincides with the *inversion method* – a standard generation method of random variables with a prescribed distribution F; see, e.g., Bratley et al. [1], Devroye [3]. Practical TES modeling usually employs composite distortions of the form

$$D = F^{-1} \circ S_\xi, \tag{2.3}$$

where the first transformation, S_ξ (called a *stitching transformation*), is selected from a family, parameterized by $0 \le \xi \le 1$, of the form

$$S_\xi(y) = \begin{cases} y/\xi, & 0 \le y < \xi \\ (1-y)/(1-\xi), & \xi \le y < 1 \end{cases} \tag{2.4}$$

It can be shown (Melamed [16], Jagerman and Melamed [7]) that the effect of each $S_\xi,\ 0 < \xi < 1$ is to "smooth" the sample paths of the background TES sequences (2.1) and (2.2). Moreover, all $S_\xi,\ 0 \le \xi \le 1$, preserve uniformity (Melamed [16]), i.e., $S_\xi(U_n)$ is also distributed uniformly on $[0,1)$. Thus, the stochastic sequences $\{X_n^+\}$ and $\{X_n^-\}$, obtained as the distorted sequences

$$X_n^+ = D(U_n^+), \quad X_n^- = D(U_n^-), \tag{2.5}$$

have general marginals. Distorted TES sequences of the form (2.5) are called *foreground* sequences and they are the target sequences in TES modeling (background sequences play an auxiliary role).

Theorems 3 and 4 (ibid.) provide numerically-computable formulas for the autocorrelation functions of $\{X_n^+\}$ and $\{X_n^-\}$, given by

$$\rho_X^+(\tau) = \frac{1}{\sigma_X^2} \sum_{\substack{\nu=-\infty \\ \nu\neq 0}}^{\infty} \tilde{f}_V^\tau(i2\pi\nu)\, |\tilde{D}(i2\pi\nu)|^2 \tag{2.6}$$

and

$$\rho_X^-(\tau) = \begin{cases} \rho_X^+(\tau), & \tau \text{ even} \\ \dfrac{1}{\sigma_X^2} \displaystyle\sum_{\substack{\nu=-\infty \\ \nu\neq 0}}^{\infty} \tilde{f}_V^\tau(i2\pi\nu)\, Re[\tilde{D}^2(i2\pi\nu)], & \tau \text{ odd,} \end{cases} \tag{2.7}$$

respectively, where $f_V^\tau(x)$ denotes the density of the τ-fold convolution of innovations $\{V_n\}$, and $i = \sqrt{-1}$. Setting $\tau = 0$ in Eq. (2.6) yields the identity

$$\sigma_X^2 \;=\; \sum_{\substack{\nu=-\infty \\ \nu\neq 0}}^{\infty} |\tilde{D}(i2\pi\nu)|^2. \tag{2.8}$$

An important subclass of TES processes corresponds to probabilistic mixtures of uniform innovations, i.e., step-function densities of the form

$$f_V(x) \;=\; \sum_{k=1}^{K} 1_{[L_k,R_k)}(x)\,\frac{P_k}{R_k - L_k}, \quad -0.5 \le x \le 0.5, \tag{2.9}$$

where K is the number of steps, $[L_k, R_k)$ is the support of step k ($-0.5 \le L_k < R_k < 0.5$), and $0 < P_k \le 1$ is the mixing probability of step k ($\sum_{k=1}^{K} P_k = 1$).

The TES modeling methodology seeks a TES model whose marginal distribution is guaranteed to match its empirical counterpart (histogram), and simultaneously, whose autocorrelation function approximates the leading empirical autocorrelations. The fitting procedure consists of a heuristic search, under software support, over stitching parameters in the range [0, 1] and step-function innovation densities of the form (2.9); see Geist and Melamed [4], Melamed et al. [18]. Computer-aided TES modeling has been used to accurately model compressed video traffic processes (Lee et al. [12], Melamed and Sengupta [17]). An algorithmic modeling approach has been recently developed for TES modeling [10]. The algorithm first carries out a brute-force computation over a subspace of step-function innovation densities and various stitching parameters. The algorithm then selects the best n combinations of pairs, (f_V, ξ), in the sense that the resulting TES model autocorrelation functions minimize the mean square error with respect to the empirical autocorrelation function. The analyst then selects among those n candidate models the one whose Monte Carlo sample paths bear the "most resemblance" to the empirical record. Experience shows that the TES modeling algorithm produces better and faster results than its heuristic counterpart.

The spectral functions of *basic* TES processes — those with single-step innovation densities ($K = 1$) and no stitching — were studied in Jagerman and Melamed [9]. The main contribution of the present paper is to extend the spectral analysis of Jagerman and Melamed [9] to TES sequences with general innovation densities and general distortions.

3 SPECTRAL FUNCTIONS FOR TES$^+$ SEQUENCES

In this section we derive numerically-computable formulas for the spectral functions $s_X^+(\omega)$ and $S_X^+(\omega)$ of a general TES$^+$ sequence $\{X_n^+\}$.

In calculating TES spectral densities we shall need the identity

$$\sum_{\tau=1}^{\infty} x^{\tau} \cos(\tau\omega) \;=\; \frac{1 - x\cos(\omega)}{1 - 2x\cos(\omega) + x^2} - 1 \;=\; \frac{1}{2}\left[\frac{1 - x^2}{1 - 2x\cos(\omega) + x^2} - 1\right], \tag{3.1}$$

valid for any complex x with $|x| < 1$ and any real ω, which is easily obtained as the real part of the geometric sum $\sum_{\tau=1}^{\infty} \left(x\, e^{i\omega}\right)^{\tau} = \frac{x\, e^{i\omega}}{1 - x\, e^{i\omega}}$.

Theorem 1 *The spectral density function $s_X^+(\omega)$ is given by*

$$s_X^+(\omega) \;=\; \frac{2}{\pi\,\sigma_X^2}\sum_{\nu=1}^{\infty} |\tilde{D}(i2\pi\nu)|^2\, Re\!\left[\frac{1 - \tilde{f}_V^2(i2\pi\nu)}{1 - 2\tilde{f}_V(i2\pi\nu)\cos(\omega) + \tilde{f}_V^2(i2\pi\nu)}\right]. \tag{3.2}$$

Proof Substituting Eq. (2.6) into Eq. (1.2) yields

$$\begin{aligned} s_X^+(\omega) \;&=\; \frac{1}{\pi} + \frac{2}{\pi\,\sigma_X^2}\sum_{\tau=1}^{\infty}\left[\sum_{\substack{\nu=-\infty \\ \nu\neq 0}}^{\infty} |\tilde{D}(i2\pi\nu)|^2\, \tilde{f}_V^{\tau}(i2\pi\nu)\right]\cos(\tau\omega) \\ &=\; \frac{1}{\pi} + \frac{2}{\pi\,\sigma_X^2}\sum_{\substack{\nu=-\infty \\ \nu\neq 0}}^{\infty} |\tilde{D}(i2\pi\nu)|^2 \sum_{\tau=1}^{\infty} \tilde{f}_V^{\tau}(i2\pi\nu)\cos(\tau\omega), \end{aligned}$$

where the order of summation may be validly interchanged by the absolute convergence of the double summation. To see that, note that $|\tilde{f}_V(i2\pi\nu)| < 1$ for $\nu \neq 0$, while the assumption $\sigma_X^2 < \infty$ and relation (2.8) ensure the finiteness of $\sum_{\substack{\nu=-\infty \\ \nu\neq 0}}^{\infty} |\tilde{D}(i2\pi\nu)|^2$ (see Knopp [11]). Next, apply to the last summation above the identity (3.1) with $x = \tilde{f}_V(i2\pi\nu)$ for each ν, yielding

$$\begin{aligned} s_X^+(\omega) \;&=\; \frac{1}{\pi} + \frac{2}{\pi\,\sigma_X^2}\sum_{\substack{\nu=-\infty \\ \nu\neq 0}}^{\infty} |\tilde{D}(i2\pi\nu)|^2\, \frac{1}{2}\left[\frac{1 - \tilde{f}_V^2(i2\pi\nu)}{1 - 2\tilde{f}_V(i2\pi\nu)\cos(\omega) + \tilde{f}_V^2(i2\pi\nu)} - 1\right] \\ &=\; \frac{1}{\pi\,\sigma_X^2}\sum_{\substack{\nu=-\infty \\ \nu\neq 0}}^{\infty} |\tilde{D}(i2\pi\nu)|^2\, \frac{1 - \tilde{f}_V^2(i2\pi\nu)}{1 - 2\tilde{f}_V(i2\pi\nu)\cos(\omega) + \tilde{f}_V^2(i2\pi\nu)}, \end{aligned} \tag{3.3}$$

where the second equality is justified by the identity (2.8). Eq. (3.2) now follows by noting that in the summation above, terms indexed by $-\nu$ and ν are complex conjugates. $\square$

In calculating TES integrated spectra we shall need the identity

$$\int_0^\omega \sum_{\tau=1}^{\infty} x^\tau \cos(\tau y)\, dy \;=\; \sum_{\tau=1}^{\infty} x^\tau \, \frac{\sin(\tau\omega)}{\tau} \;=\; \tan^{-1}\!\left(\frac{1+x}{1-x}\,\tan\!\left(\frac{\omega}{2}\right)\right) - \frac{\omega}{2}, \quad (3.4)$$

valid for any complex x with $|x| < 1$ and any real ω, which is obtained from Eq. (3.1) by integration.

Theorem 2 *The integrated spectrum function $S_X^+(\omega)$ is given by*

$$S_X^+(\omega) \;=\; \frac{4}{\pi\, \sigma_X^2} \sum_{\nu=1}^{\infty} |\tilde{D}(i2\pi\nu)|^2 \, Re\!\left[\tan^{-1}\!\left(\frac{1+\tilde{f}_V(i2\pi\nu)}{1-\tilde{f}_V(i2\pi\nu)}\,\tan\!\left(\frac{\omega}{2}\right)\right)\right]. \quad (3.5)$$

Proof Substituting Eq. (2.6) into Eq. (1.3) yields

$$\begin{aligned} S_X^+(\omega) \;&=\; \frac{\omega}{\pi} \;+\; \frac{2}{\pi\, \sigma_X^2} \sum_{\tau=1}^{\infty} \Bigg[\sum_{\substack{\nu=-\infty \\ \nu\neq 0}}^{\infty} |\tilde{D}(i2\pi\nu)|^2 \, \tilde{f}_V^\tau(i2\pi\nu) \Bigg] \frac{\sin(\tau\omega)}{\tau} \\ &=\; \frac{\omega}{\pi} \;+\; \frac{2}{\pi\, \sigma_X^2} \sum_{\substack{\nu=-\infty \\ \nu\neq 0}}^{\infty} |\tilde{D}(i2\pi\nu)|^2 \sum_{\tau=1}^{\infty} \tilde{f}_V^\tau(i2\pi\nu) \, \frac{\sin(\tau\omega)}{\tau}, \end{aligned}$$

where, as in Theorem 1, the order of summation may be validly interchanged by the absolute convergence of the double summation. Next, apply to the last summation above the identity (3.4) with $x = \tilde{f}_V(i2\pi\nu)$ for each ν, yielding

$$\begin{aligned} S_X^+(\omega) \;&=\; \frac{\omega}{\pi} \;+\; \frac{2}{\pi\, \sigma_X^2} \sum_{\substack{\nu=-\infty \\ \nu\neq 0}}^{\infty} |\tilde{D}(i2\pi\nu)|^2 \left[\tan^{-1}\!\left(\frac{1+\tilde{f}_V(i2\pi\nu)}{1-\tilde{f}_V(i2\pi\nu)}\,\tan\!\left(\frac{\omega}{2}\right)\right) - \frac{\omega}{2}\right] \\ &=\; \frac{2}{\pi\, \sigma_X^2} \sum_{\substack{\nu=-\infty \\ \nu\neq 0}}^{\infty} |\tilde{D}(i2\pi\nu)|^2 \, \tan^{-1}\!\left(\frac{1+\tilde{f}_V(i2\pi\nu)}{1-\tilde{f}_V(i2\pi\nu)}\,\tan\!\left(\frac{\omega}{2}\right)\right), \end{aligned} \quad (3.6)$$

where the second equality is justified by the identity (2.8). Eq. (3.5) now follows by noting that $\tan^{-1}(x)$ is real for x real, and that terms indexed by $-\nu$ and ν, in the summation above, are complex conjugates. $\square$

While providing compact representations for TES$^+$ spectral formulas, Eq. (3.2) in Theorem 1 and Eq. (3.5) in Theorem 2 are not optimized for computational speed. Computationally-enhanced versions thereof can be obtained by modifying each case so as to cause the infinite summations to converge faster.

Proposition 1 *Alternative fast-converging representations for TES$^+$ spectral functions are given by*

$$s_X^+(\omega) \;=\; \frac{1}{\pi} \;+\; \frac{2}{\pi\,\sigma_X^2}\sum_{\nu=1}^{\infty}|\tilde{D}(i2\pi\nu)|^2\,Re\left[\frac{1-\tilde{f}_V^2(i2\pi\nu)}{1-2\tilde{f}_V(i2\pi\nu)\cos(\omega)+\tilde{f}_V^2(i2\pi\nu)}-1\right] \tag{3.7}$$

$$S_X^+(\omega) \;=\; \frac{\omega}{\pi} \;+\; \frac{4}{\pi\,\sigma_X^2}\sum_{\nu=1}^{\infty}|\tilde{D}(i2\pi\nu)|^2\,Re\left[\tan^{-1}\left(\frac{1+\tilde{f}_V(i2\pi\nu)}{1-\tilde{f}_V(i2\pi\nu)}\,\tan\left(\frac{\omega}{2}\right)\right)-\frac{\omega}{2}\right] \tag{3.8}$$

Proof Eq. (3.7) follows from the first equality in Eq. (3.3), while Eq. (3.8) follows from the first equality in Eq. (3.6), since in both cases, terms indexed by $-\nu$ and ν in the corresponding infinite sums are complex conjugates.

Next, consider the two equalities in Eq. (3.3). Note that the summands, in each infinite sum, constitute products of two factors. The first factor is $|\tilde{D}(i2\pi\nu)|^2$ which converges to zero as $\nu \uparrow \infty$. However, the (bracketed) second factor converges to zero in the first equality as $\nu \uparrow \infty$, whereas its counterpart in the second equality converges to one. Clearly the products in the first equality converge faster to zero than the corresponding products in the second equality, thereby establishing that Eq. (3.7) converges faster than Eq. (3.2).

Finally, consider the two equalities in Eq. (3.6). A similar convergence argument applies to corresponding factors in the respective infinite sums. Again the (bracketed) second factor converges to zero in the first equality as $\nu \uparrow \infty$, whereas its counterpart in the second equality converges to $\frac{\omega}{2}$, thereby establishing that Eq. (3.8) converges faster than Eq. (3.5). □

Figures 1 and 2 illustrate graphs of TES$^+$ spectral densities, obtained via a numerical calculation of Eq. (1.6), based on Eq. (3.7). A detailed discussion of these examples is deferred until Section 6.

4 SPECTRAL FUNCTIONS FOR TES$^-$ SEQUENCES

In this section we derive numerically-computable formulas for the spectral functions $s_X^-(\omega)$ and $S_X^-(\omega)$ of a general TES$^-$ sequence $\{X_n^-\}$. To this end, write $\tilde{D}(i2\pi\nu) = a_\nu + i\,b_\nu$ for $\nu \geq 1$, so that

$$|\tilde{D}(i2\pi\nu)|^2 \;=\; a_\nu^2 + b_\nu^2, \quad Re[\tilde{D}^2(i2\pi\nu)] \;=\; a_\nu^2 - b_\nu^2. \tag{4.1}$$

Theorem 3 *The spectral density function $s_X^-(\omega)$ is given by*

$$\begin{aligned} s_X^-(\omega) \;=\;& \frac{2}{\pi\,\sigma_X^2} \sum_{\nu=1}^{\infty} a_\nu^2\, Re\left[\frac{1-\tilde{f}_V^2(i2\pi\nu)}{1-2\tilde{f}_V(i2\pi\nu)\cos(\omega)+\tilde{f}_V^2(i2\pi\nu)}\right] \\ &+\; \frac{2}{\pi\,\sigma_X^2} \sum_{\nu=1}^{\infty} b_\nu^2\, Re\left[\frac{1-\tilde{f}_V^2(i2\pi\nu)}{1+2\tilde{f}_V(i2\pi\nu)\cos(\omega)+\tilde{f}_V^2(i2\pi\nu)}\right]. \end{aligned} \tag{4.2}$$

Proof Substituting Eq. (2.7) into Eq. (1.2) yields

$$\begin{aligned} s_X^-(\omega) \;=\;& \frac{1}{\pi} \;+\; \frac{2}{\pi}\sum_{k=1}^{\infty} \rho_X^+(2k)\cos(2k\omega) \;+\; \frac{2}{\pi}\sum_{k=1}^{\infty} \rho_X^-(2k-1)\cos((2k-1)\omega) \\ =\;& \frac{1}{\pi} \;+\; \frac{2}{\pi\,\sigma_X^2}\sum_{k=1}^{\infty}\left[\sum_{\substack{\nu=-\infty\\ \nu\neq 0}}^{\infty} |\tilde{D}(i2\pi\nu)|^2\, \tilde{f}_V^{2k}(i2\pi\nu)\right]\cos(2k\omega) \\ &+\; \frac{2}{\pi\,\sigma_X^2}\sum_{k=1}^{\infty}\left[\sum_{\substack{\nu=-\infty\\ \nu\neq 0}}^{\infty} Re[\tilde{D}^2(i2\pi\nu)]\, \tilde{f}_V^{2k-1}(i2\pi\nu)\right]\cos((2k-1)\omega). \end{aligned}$$

As in Theorem 1, the double summations above are absolutely convergent, so interchanging the order of summations and using the representations in (4.1), yield

$$\begin{aligned} s_X^-(\omega) \;=\;& \frac{1}{\pi} \;+\; \frac{2}{\pi\,\sigma_X^2}\sum_{\substack{\nu=-\infty\\ \nu\neq 0}}^{\infty} (a_\nu^2 + b_\nu^2)\sum_{k=1}^{\infty} \tilde{f}_V^{2k}(i2\pi\nu)\cos(2k\omega) \\ &+\; \frac{2}{\pi\,\sigma_X^2}\sum_{\substack{\nu=-\infty\\ \nu\neq 0}}^{\infty} (a_\nu^2 - b_\nu^2)\sum_{k=1}^{\infty} \tilde{f}_V^{2k-1}(i2\pi\nu)\cos((2k-1)\omega) \\ =\;& \frac{1}{\pi} \;+\; \frac{2}{\pi\,\sigma_X^2}\sum_{\substack{\nu=-\infty\\ \nu\neq 0}}^{\infty} a_\nu^2 \sum_{k=1}^{\infty} \tilde{f}_V^{k}(i2\pi\nu)\cos(k\omega) \\ &+\; \frac{2}{\pi\,\sigma_X^2}\sum_{\substack{\nu=-\infty\\ \nu\neq 0}}^{\infty} b_\nu^2 \sum_{k=1}^{\infty} [-\tilde{f}_V(i2\pi\nu)]^{k}\cos(k\omega). \end{aligned}$$

Next, apply the identity (3.1) in the two summations above with $x = \tilde{f}_V(i2\pi\nu)$ and $x = -\tilde{f}_V(i2\pi\nu)$, respectively, for each ν, as in Theorem 1, whence

$$\begin{aligned} s_X^-(\omega) &= \frac{1}{\pi} + \frac{2}{\pi\,\sigma_X^2} \sum_{\substack{\nu=-\infty \\ \nu\neq 0}}^{\infty} a_\nu^2 \,\frac{1}{2} \left[\frac{1-\tilde{f}_V^2(i2\pi\nu)}{1-2\tilde{f}_V(i2\pi\nu)\cos(\omega)+\tilde{f}_V^2(i2\pi\nu)} - 1 \right] \\ &\quad + \frac{2}{\pi\,\sigma_X^2} \sum_{\substack{\nu=-\infty \\ \nu\neq 0}}^{\infty} b_\nu^2 \,\frac{1}{2} \left[\frac{1-\tilde{f}_V^2(i2\pi\nu)}{1+2\tilde{f}_V(i2\pi\nu)\cos(\omega)+\tilde{f}_V^2(i2\pi\nu)} - 1 \right] \\ &= \frac{1}{\pi\,\sigma_X^2} \sum_{\substack{\nu=-\infty \\ \nu\neq 0}}^{\infty} a_\nu^2 \left[\frac{1-\tilde{f}_V^2(i2\pi\nu)}{1-2\tilde{f}_V(i2\pi\nu)\cos(\omega)+\tilde{f}_V^2(i2\pi\nu)} \right] \\ &\quad + \frac{1}{\pi\,\sigma_X^2} \sum_{\substack{\nu=-\infty \\ \nu\neq 0}}^{\infty} b_\nu^2 \left[\frac{1-\tilde{f}_V^2(i2\pi\nu)}{1+2\tilde{f}_V(i2\pi\nu)\cos(\omega)+\tilde{f}_V^2(i2\pi\nu)} \right], \end{aligned} \tag{4.3}$$

where the second equality is justified by the identity (2.8). Eq. (4.2) now follows by noting that terms indexed by $-\nu$ and ν in each summation above are complex conjugates. □

Theorem 4 *The integrated spectrum function $S_X^-(\omega)$ is given by*

$$\begin{aligned} S_X^-(\omega) &= \frac{4}{\pi\,\sigma_X^2} \sum_{\nu=1}^{\infty} a_\nu^2 \, Re\left[\tan^{-1}\left(\frac{1+\tilde{f}_V(i2\pi\nu)}{1-\tilde{f}_V(i2\pi\nu)} \tan\left(\frac{\omega}{2}\right) \right) \right] \\ &\quad + \frac{4}{\pi\,\sigma_X^2} \sum_{\nu=1}^{\infty} b_\nu^2 \, Re\left[\tan^{-1}\left(\frac{1-\tilde{f}_V(i2\pi\nu)}{1+\tilde{f}_V(i2\pi\nu)} \tan\left(\frac{\omega}{2}\right) \right) \right]. \end{aligned} \tag{4.4}$$

Proof Substituting Eq. (2.7) into Eq. (1.3), similarly to Theorem 3, yields

$$\begin{aligned} S_X^-(\omega) &= \frac{\omega}{\pi} + \frac{2}{\pi} \sum_{k=1}^{\infty} \rho_X^+(2k) \frac{\sin(2k\omega)}{2k} + \frac{2}{\pi} \sum_{k=1}^{\infty} \rho_X^-(2k-1) \frac{\sin((2k-1)\omega)}{2k-1} \\ &= \frac{\omega}{\pi} + \frac{2}{\pi\,\sigma_X^2} \sum_{\substack{\nu=-\infty \\ \nu\neq 0}}^{\infty} (a_\nu^2 + b_\nu^2) \sum_{k=1}^{\infty} \tilde{f}_V^{2k}(i2\pi\nu) \frac{\sin(2k\omega)}{2k} \\ &\quad + \frac{2}{\pi\,\sigma_X^2} \sum_{\substack{\nu=-\infty \\ \nu\neq 0}}^{\infty} (a_\nu^2 - b_\nu^2) \sum_{k=1}^{\infty} \tilde{f}_V^{2k-1}(i2\pi\nu) \frac{\sin((2k-1)\omega)}{2k-1} \\ &= \frac{\omega}{\pi} + \frac{2}{\pi\,\sigma_X^2} \sum_{\substack{\nu=-\infty \\ \nu\neq 0}}^{\infty} a_\nu^2 \sum_{k=1}^{\infty} \tilde{f}_V^{k}(i2\pi\nu) \frac{\sin(k\omega)}{k} \\ &\quad + \frac{2}{\pi\,\sigma_X^2} \sum_{\substack{\nu=-\infty \\ \nu\neq 0}}^{\infty} b_\nu^2 \sum_{k=1}^{\infty} [-\tilde{f}_V(i2\pi\nu)]^k \frac{\sin(k\omega)}{k}. \end{aligned}$$

Next, apply the identity (3.4) in the two summations above with $x = \tilde{f}_V(i2\pi\nu)$ and $x = -\tilde{f}_V(i2\pi\nu)$, respectively, for each ν, whence

$$\begin{aligned} S_X^-(\omega) &= \frac{\omega}{\pi} + \frac{2}{\pi\,\sigma_X^2} \sum_{\substack{\nu=-\infty \\ \nu\neq 0}}^{\infty} a_\nu^2 \left[\tan^{-1}\!\left(\frac{1+\tilde{f}_V(i2\pi\nu)}{1-\tilde{f}_V(i2\pi\nu)}\,\tan\!\left(\frac{\omega}{2}\right)\right) - \frac{\omega}{2}\right] \\ &\quad + \frac{2}{\pi\,\sigma_X^2} \sum_{\substack{\nu=-\infty \\ \nu\neq 0}}^{\infty} b_\nu^2 \left[\tan^{-1}\!\left(\frac{1-\tilde{f}_V(i2\pi\nu)}{1+\tilde{f}_V(i2\pi\nu)}\,\tan\!\left(\frac{\omega}{2}\right)\right) - \frac{\omega}{2}\right] \\ &= \frac{2}{\pi\,\sigma_X^2} \sum_{\substack{\nu=-\infty \\ \nu\neq 0}}^{\infty} a_\nu^2 \tan^{-1}\!\left(\frac{1+\tilde{f}_V(i2\pi\nu)}{1-\tilde{f}_V(i2\pi\nu)}\,\tan\!\left(\frac{\omega}{2}\right)\right) \\ &\quad + \frac{2}{\pi\,\sigma_X^2} \sum_{\substack{\nu=-\infty \\ \nu\neq 0}}^{\infty} b_\nu^2 \tan^{-1}\!\left(\frac{1-\tilde{f}_V(i2\pi\nu)}{1+\tilde{f}_V(i2\pi\nu)}\,\tan\!\left(\frac{\omega}{2}\right)\right), \end{aligned} \tag{4.5}$$

where the second equality is justified by the identity (2.8). Eq. (4.2) now follows by noting that $\tan^{-1}(x)$ is real for x real, and that terms indexed by $-\nu$ and ν, in the summations above, are complex conjugates. □

Computationally-enhanced versions of the TES$^-$ spectral functions, Eqs. (4.2) and (4.4), can be obtained analogously to Proposition 1.

Proposition 2 *Alternative fast-converging representations for TES$^-$ spectral functions are given by*

$$\begin{aligned} s_X^-(\omega) &= \frac{1}{\pi} + \frac{2}{\pi\,\sigma_X^2} \sum_{\nu=1}^{\infty} a_\nu^2\, Re\left[\frac{1-\tilde{f}_V^2(i2\pi\nu)}{1-2\tilde{f}_V(i2\pi\nu)\cos(\omega)+\tilde{f}_V^2(i2\pi\nu)} - 1\right] \\ &\quad + \frac{2}{\pi\,\sigma_X^2} \sum_{\nu=1}^{\infty} b_\nu^2\, Re\left[\frac{1-\tilde{f}_V^2(i2\pi\nu)}{1+2\tilde{f}_V(i2\pi\nu)\cos(\omega)+\tilde{f}_V^2(i2\pi\nu)} - 1\right] \end{aligned} \tag{4.6}$$

$$\begin{aligned} S_X^-(\omega) &= \frac{\omega}{\pi} + \frac{4}{\pi\,\sigma_X^2} \sum_{\nu=1}^{\infty} a_\nu^2\, Re\left[\tan^{-1}\left(\frac{1+\tilde{f}_V(i2\pi\nu)}{1-\tilde{f}_V(i2\pi\nu)}\,\tan\!\left(\frac{\omega}{2}\right)\right) - \frac{\omega}{2}\right] \\ &\quad + \frac{4}{\pi\,\sigma_X^2} \sum_{\nu=1}^{\infty} b_\nu^2\, Re\left[\tan^{-1}\left(\frac{1-\tilde{f}_V(i2\pi\nu)}{1+\tilde{f}_V(i2\pi\nu)}\,\tan\!\left(\frac{\omega}{2}\right)\right) - \frac{\omega}{2}\right] \end{aligned} \tag{4.7}$$

Proof Completely analogous to that of Proposition 1. □

Figures 3 and 4 illustrate graphs of TES$^-$ spectral densities, obtained via a numerical calculation of Eq. (1.6), based on Eq. (4.6). A detailed discussion of these examples is deferred until Section 6.

5 THE MIRROR-IMAGE PROPERTY

We say that TES processes $\{X_n^+\}$ and $\{X_n^-\}$ are *compatible*, if they have the same innovation and distortion. A pair of compatible TES processes is said to satisfy the *mirror-image property*, provided

$$s_X^+(\omega) = s_X^-(\pi - \omega), \quad \omega \in [0, \pi]. \tag{5.1}$$

In other words, the mirror image property means that s_X^- can be obtained from s_X^+ (and vice versa) by a symmetrical "reflection" operation about the point $\frac{\pi}{2}$, as exemplified in Figures 1 and 3.

Jagerman and Melamed [9] showed that the mirror-image property (5.1) holds for basic TES processes with uniform marginals and no stitching; see Eqs. (5.4) and (5.5), *ibid*. The next theorem extends this result to general TES processes.

Theorem 5 *Any pair of compatible TES processes* $\{X_n^+\}$ *and* $\{X_n^-\}$ *satisfy (5.1), provided*

$$a_\nu = 0, \quad \nu \geq 1. \tag{5.2}$$

Proof Follows immediately from the spectral representations (3.2) and (4.2), by noting that $\cos(\omega) = -\cos(\pi - \omega)$. □

Note that Condition (5.2) means that

$$a_\nu \; = \; \int_0^1 D(x)\, cos(2\pi\nu x)\, dx \; = \; 0. \tag{5.3}$$

A direct calculation shows that Eq. (5.3) holds, in particular, for any linear distortion of the form

$$D(x) \; = \; cx \; + \; d. \tag{5.4}$$

See also Eq. (3.12) in Jagerman and Melamed [8].

Examples of compatible TES processes with and without the mirror-image property are further discussed in Section 6.

6 DISCUSSION

In order to gauge the efficacy of the formulas for TES spectral densities, we compared their numerically-computed values against their simulation-based estimates. Sample results are displayed in Figures 1 – 4. The solid lines correspond to the Hertz spectral densities $s_X^*(f)$ of Eq. (1.6), computed from Eqs. (3.7) and (4.6). The bullets correspond to the associated simulation-based statistical estimates, computed via Eq. (1.7), with $m = 10^3$, from Monte Carlo simulations of 10^6 observations each. A two-step innovation density with parameters $(L_1 = -0.1, R_1 = 0.2, P_1 = 0.5)$ and $(L_2 = 0.2, R_2 = 0.4, P_2 = 0.5)$ was used in all cases, while the distortions employed were uniform (with the null stitching parameter $\xi = 1$) and exponential (with stitching parameter $\xi = 0.25$). Observe that each pair of corresponding curves has the same functional form and is generally in good agreement.

Figures 1 and 2 display the spectral densities for TES$^+$ processes. Notice that the overall functional form has not been greatly altered under the exponential distortion and stitching. On the other hand, the corresponding TES$^-$ spectral densities in Figures 3 and 4 exhibit considerable functional differences. Experience has shown that TES$^-$ has a more complex spectral structure than TES$^+$.

Figures 1 and 3 confirm the mirror-image property (5.1). Note that background TES processes correspond to the trivial linear case $D = I$ (the identity), with purely imaginary $\tilde{D}(i2\pi\nu)$ of the form

$$\tilde{D}(i2\pi\nu) \;=\; \frac{i}{2\pi\nu}, \tag{6.1}$$

which satisfies the mirror-image sufficiency condition (5.3). We note in passing that (5.3) will also hold if $D(x)$ is anti-symmetric about $\frac{1}{2}$ in the sense that $D(\frac{1}{2}+x) = -D(\frac{1}{2}-x)$, for $x \in [0, \frac{1}{2}]$. In contrast, a visual inspection of Figures 2 and 4 reveals that they fail to satisfy the mirror image relation. Indeed, the corresponding TES processes fail to satisfy the sufficiency condition (5.2) since the logarithmic inversion and stitching used do not yield purely imaginary quantities $\tilde{D}(i2\pi\nu) = ib_\nu$; see Proposition 8 in Jagerman and Melamed [8].

Additional examples of TES spectral functions, drawn from the subclass of basic TES processes, may be found in Jagerman and Melamed [9].

Finally, we remark on the functional form of second-order statistics engendered by TES sequences. Both the TES autocorrelation functions (2.6) and (2.7), as well as the spectral functions (3.2), (3.5), (4.2) and (4.4), are generally represented by infinite sums involving the Laplace transforms of the associated distortion transformation and innovation density. These infinite sums can have a variety of functional forms whose character is not readily evident from their formal representations. When the infinite sums reduce to finite sums, however, we get explicit closed-form expressions. In particular, this happens when either the distortion transformation or the innovation density (or both) are trigonometric polynomials (Natanson [19]), that is, functions of the form

$$T(x) \;=\; \sum_{\nu=-s}^{s} \tilde{T}(i2\pi\nu)\, e^{i2\pi\nu x}$$

for some finite integer $s \geq 0$. The reduction to finite sums then follows from the fact that trigonometric polynomials satisfy $\tilde{T}(i2\pi\nu) = 0$ for $|\nu| > s$. Interestingly, the corresponding TES autocorrelation functions (2.6) and (2.7) reduce then to weighted sums of powers, sometimes encountered in linear autoregressive (AR) processes.

Acknowledgments

We thank A. Merchant for reading and commenting on this paper. Special thanks are due to S.Q. Li for elucidating his frequency domain approach.

References

[1] Bratley, P., Fox B.L. and Schrage, L.E., *A Guide to Simulation*, Springer-Verlag, 1987.

[2] Cox, D.R. and Lewis, P.A.W., *The Statistical Analysis of Series of Events*, Methuen and Co., London, 1968.

[3] Devroye, L., *Non-Uniform Random Variate Generation*, Springer-Verlag, 1986.

[4] Geist, D. and Melamed, B., "TEStool: An Environment for Visual Interactive Modeling of Autocorrelated Traffic", *Proceedings of the 1992 International Conference on Communications* (Chicago, Illinois). Vol. 3, 1285–1289, 1992.

[5] Grenander, U. and Rosenblatt, M., *Statistical Analysis of Stationary Time Series*, Wiley, 1957.

[6] Hamming, R.W., *Digital Filters*, Prentice-Hall, 1989.

[7] Jagerman, D.L. and Melamed, B., “The Transition and Autocorrelation Structure of TES Processes Part I: General Theory,” *Stochastic Models*, Vol. 8, No. 2, 193–219, 1992.

[8] Jagerman, D.L. and Melamed, B., “The Transition and Autocorrelation Structure of TES Processes Part II: Special Cases,” *Stochastic Models*, Vol. 8, No. 3, 499–527, 1992.

[9] Jagerman, D.L. and Melamed, B., “Spectral Analysis of Basic TES Processes”, *ORSA J. on Computing*, to appear, 1993.

[10] Jelenkovic, P., Melamed, B. and Sengupta, B., "Algorithmic Modeling of TES Processes", manuscript in preparation, NEC USA Inc, Princeton, New Jersey, 1994.

[11] Knopp, K., *Theory and Application of Infinite Series*, Blackie and Son, London and Glasgow, 1946.

[12] Lee, D.-S., Melamed, B., Reibman A. and Sengupta, B., "TES Modeling for Analysis of a Video Multiplexor", *Performance Evaluation*, Vol. 16, 21–34, 1992.

[13] Li, S.Q. and Hwang, C.L., "Queue Response to Input Correlation Functions: Discrete Spectral Analysis," *IEEE/ACM Trans. Networking*, Vol. 1, No. 5, 522–533, 1993.

[14] Li, S.Q. and Hwang, C.L., "Queue Response to Input Correlation Functions: Continuous Spectral Analysis," *IEEE/ACM Trans. on Networking*, Vol. 1, No. 6, 1993.

[15] Livny, M., Melamed, B. and Tsiolis, A.K., "The Impact of Autocorrelation on Queueing Systems," *Management Science*, Vol. 39, No. 3, 322–339, 1993.

[16] Melamed, B., "TES: A Class of Methods for Generating Autocorrelated Uniform Variates," *ORSA J. on Computing*, Vo. 3, No. 4, 317–329, 1991.

[17] Melamed, B. and Sengupta, B., "TES modeling of video traffic", *IEICE Transactions on Communications*, Vol. E75-B, No. 12, 1291–1300, 1992.

[18] Melamed, B., Goldsman, D. and Hill, J.R., "The TES Methodology: Nonparametric Modeling of Stationary Time Series", *Proceedings of the 1992 Winter Simulation Conference*, Arlington, Virginia, 135–144, 1992.

[19] Natanson, I.P., *Constructive Function Theory*, Vol. I, Frederick Ungar Publishing Co., New York, 1964.

[20] Sheng, H.D. and Li, S.Q., "Spectral Analysis of Packet Loss Rate at Statistic Multiplexer for Multimedia Services," *IEEE Trans. on Networking*, Vol. 2, No. 1, 1994.

[21] Sheng, H.D. and Li, S.Q., "Second Order Effect of Binary Sources on Characteristics of Queue and Loss Rate," *IEEE Trans. on Communications*, Vol. 42, No. 3, 1994.

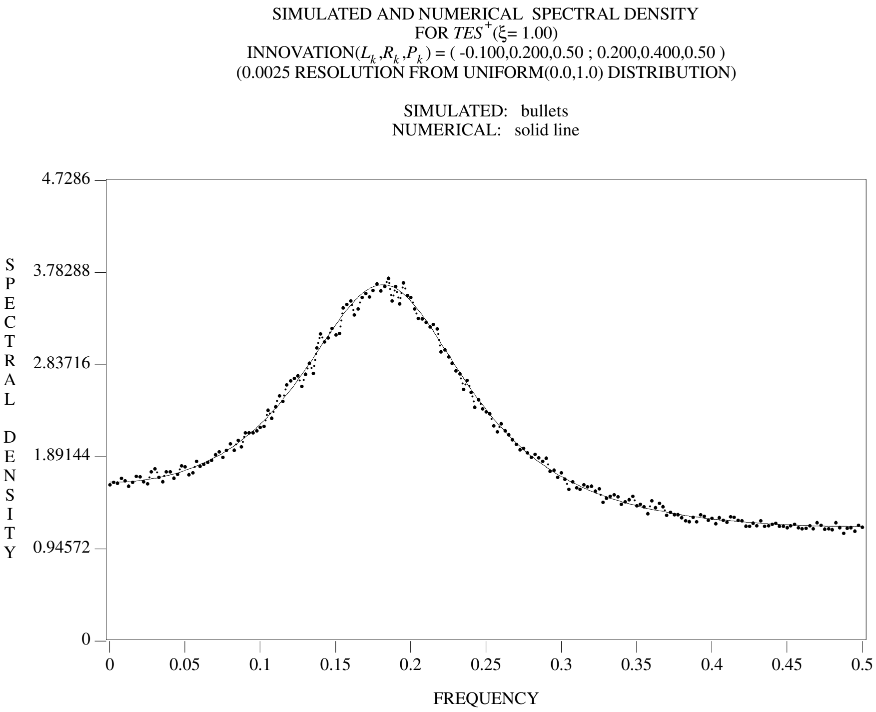

Figure 1: Spectral Densities of a Uniform TES^{+} Process

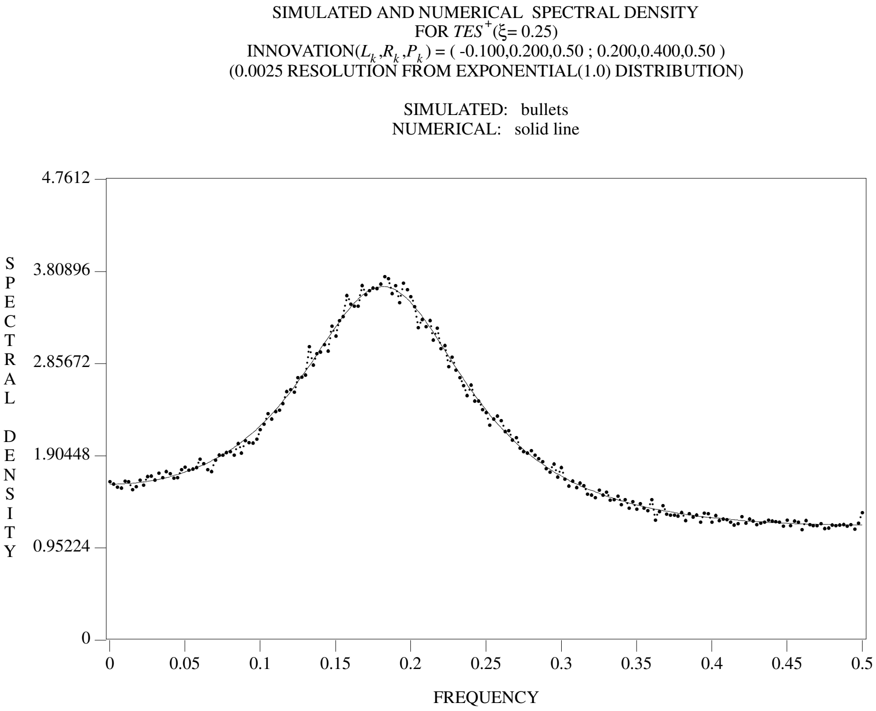

Figure 2: Spectral Densities of an Exponential TES^{+} Process

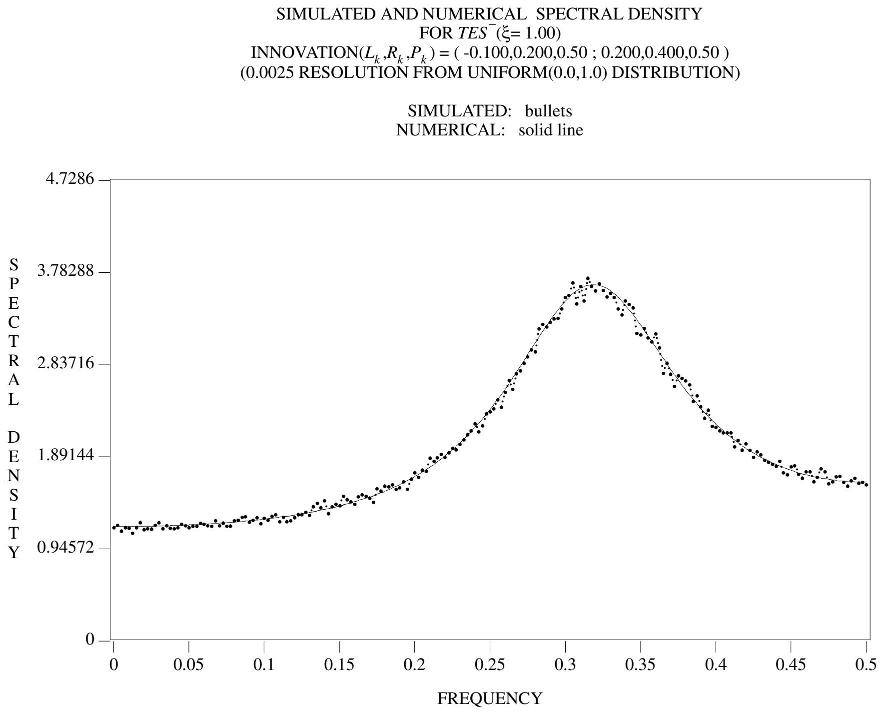

Figure 3: Spectral Densities of a Uniform TES^{-} Process

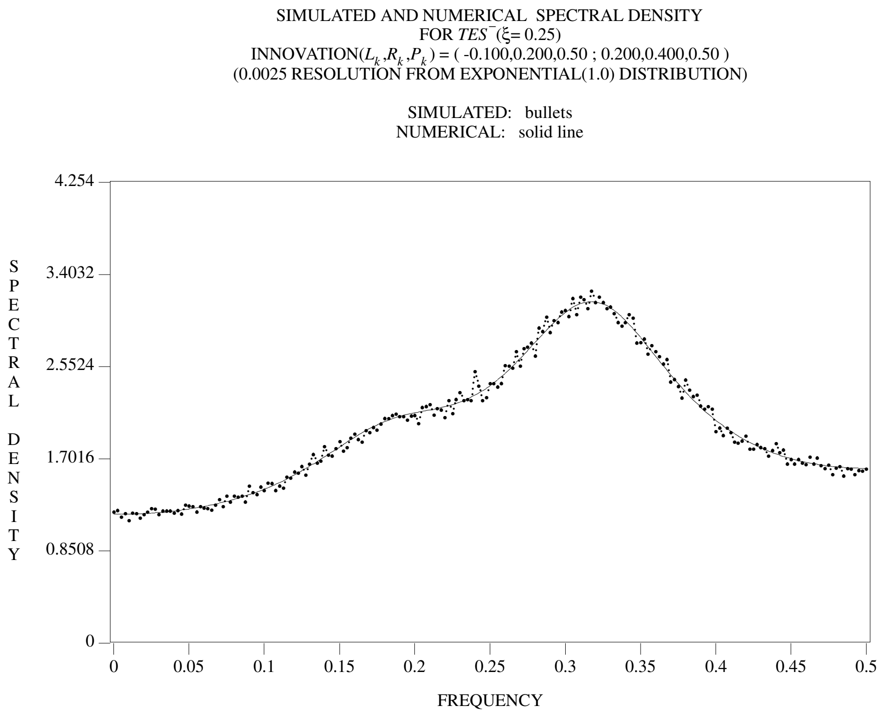

Figure 4: Spectral Densities of an Exponential TES^{-} Process